RSC Advances

PAPER

View Article Online
View Journal | View Issue



Cite this: *RSC Adv.*, 2023, **13**, 12092

# Effect and mechanism of polysilazane and platinum on tracking and erosion resistance of silicone rubber

Wanjuan Chen, *[ab] Ying Cai,[a] Jiawei Zheng,[a] Shuyan Mai,[a] Zishan Li[a] and Min Zhang[ab]

Polysilazane (PSiN) and platinum (Pt) were used to enhance the tracking and erosion resistance of silicone rubber. The suppression effects of PSiN and Pt on tracking and erosion were investigated using an inclined plane test (IPT), thermogravimetry, thermogravimetry-Fourier transform infrared spectrometry, scanning electron microscopy and laser Raman spectroscopy. It was determined that the addition of 1.8–2.4 part per hundred parts of rubber (phr) of PSiN and 8 ppm of Pt significantly enhanced the tracking and erosion resistance of silicone rubber, whereby the test specimens passed a 4.5 kV IPT with a low eroded mass and undamaged surfaces. This was attributed to the synergistic effect of PSiN and Pt on silicone chains. At high temperatures and produced by arc discharge, PSiN/Pt-catalysed radical crosslinking suppressed the degradation of silicone chains. Furthermore, the formation of a tightly crosslinked network protected the inner materials from arc ablation. In addition, carbon deposition was prevented by PSiN/Pt, making it harder for tracking to develop.

Received 10th March 2023
Accepted 13th April 2023

DOI: 10.1039/d3ra01578e

rsc.li/rsc-advances



## Introduction

Owing to its lightweight nature, weatherability, hydrophobicity and hydrophobicity recovery, silicone rubber is gradually replacing conventional ceramic and glass materials in the field of high-voltage insulation.[1,2] However, silicone rubber can suffer from tracking and erosion under arc discharge.[3] Arc discharge can easily occur on the contaminated surfaces of silicone rubber under electrical stress.[4] Repeated arc discharge contributes to the formation of a hot spot, and the high temperature leads to the thermal degradation and carbonisation of silicone rubber.[5] Consequently, tracking and erosion of silicone rubber occur, followed by insulation failure.[6]

A traditional method for improving the tracking and erosion resistance of silicone rubber is incorporating inorganic fillers, such as alumina trihydrate (ATH),[7,8] silica,[9–11] alumina[12] and boron nitride.[13] Silicone chains incorporated with these fillers are diluted and immobilised on the surface of the filler.[14] Moreover, the high thermal conductivity of inorganic fillers can facilitate heat dissipation,[15] thus enhancing the thermal stability of silicone rubber. In particular, when ATH suffers from heat, it decomposes and releases water, which react with carbon and suppresses its deposition,[16] thus retarding the tracking of the silicone rubber. However, a large loading content of inorganic fillers is required to obtain satisfactory tracking and erosion resistance.[17] As a result, the mechanical properties, surface characteristics and processability are seriously reduced, which limits the application of silicone rubber insulation materials.

Other solutions include adding an organic additive that releases arc-quenching compounds under arc discharge. For example, it has been reported that after incorporating melamine cyanurate with 15 part per hundred parts of rubber (phr) and silica, silicone rubber passed the inclined plane test (IPT) at 4.5 kV.[18,19] However, melamine cyanurate showed poor compatibility with silicone rubber, which led to its poor mechanical properties. Urea-containing silane can efficiently improve the tracking and erosion resistance of addition-cure liquid silicone rubber, along with good compatibility with silicone chains.[20,21] Nevertheless, urea-containing silane cannot improve the tracking and erosion resistance of high-temperature vulcanised silicone rubber. Our previous work showed that nitrogen-containing silane with platinum had a significant effect on the tracking and erosion resistance of silicone rubber.[22,23] Nevertheless, the polarity of nitrogen-containing silane led to migration loss in the silicone rubber matrix and reduced the performance stability of the silicone rubber. To solve this issue, we adopted polysilazane (PSiN) to cooperate with platinum (Pt) to improve the tracking and erosion resistance of silicone rubber. PSiN shares a similar molecular structure with silicone chains, which contributes to

[a]*School of Materials Science and Hydrogen Energy, Foshan University, Foshan, 528000, People's Republic of China. E-mail: wanj.chen@hotmail.com*
[b]*Guangdong Key Laboratory for Hydrogen Energy Technologies, Foshan, 528000, People's Republic of China*

good compatibility. In addition, the Si–CH=$CH_2$ and Si–H groups in PSiN can graft into the silicone chains. Thus, PSiN exhibits good dispersion and stability in the silicone rubber matrix.

In this study, PSiN and Pt were added to silicone rubber. The influence of PSiN on the tracking and erosion resistance and thermal stability of the silicone rubber was studied *via* an IPT and thermogravimetry (TG), respectively. The pyrolysis gases of the silicone rubber were characterised by thermogravimetry-Fourier transform infrared spectrometry (TG-FTIR). The morphology and characterisation of the silicone rubber after IPT were investigated by scanning electron microscopy (SEM) and laser Raman spectroscopy (LRS), respectively. Thus, a suppression mechanism for PSiN and Pt on the tracking and erosion of silicone rubber was proposed.

# Experimental

### Materials

Silicone rubber masterbatch (commercial code: SR1805) containing 27 wt% fumed silica was obtained from Shenzhen Square Silicone Group Co. Ltd, China, as was 2,5-bis(*tert*-butylperoxy)-2,5-dimethylhexane (DBPMH). Karstedt catalyst, namely platinum(0)-1,3-divinyl-1,1,3,3-tetramethylsiloxane (3300 ppm Pt), was purchased from Dongguan Batterly Materials Co. Ltd, China. PSiN was purchased from Beyond Industries Co. Ltd, China. The chemical structure of PSiN was determined by FTIR and $^1$H nuclear magnetic resonance ($^1$H-NMR), as reported in our previous study.[24] The molecular structure of PSiN is shown in Fig. 1 and $a:b:c = 1:0.37:3.76$, according to $^1$H-NMR result. The number-average molecular weight of PSiN was 1617 g mol$^{-1}$ and polydispersity index was 1.53, according to gel permeation chromatograph (GPC) result.

### Preparation of silicone rubber samples

PSiN, Karstedt catalyst and DBPMH were successively introduced into a silicone rubber masterbatch on a two-roll mill. The obtained mixture was then compression moulded (8 MPa and 165 °C) for 20 min to 120 × 50 × 6 mm$^3$. Secondary vulcanisation was then undertaken at 180 °C for 4 h. The mixing formulas of the silicone rubber samples are shown in Table 1.

### Testing and characterisation

A Waters 2410 gel permeation chromatograph (Waters, USA) was employed to test the molecular weight and molecular weight distribution of PSiN. Monodisperse polystyrene was used as the standard sample. The eluent was tetrahydrofuran.

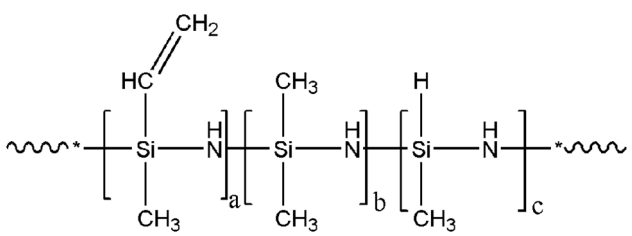


Fig. 1 Molecular structure of polysilazane.

Table 1 Formulation of silicone rubber samples[a]

| Sample codes | Silicone rubber masterbatch (g) | PSiN (phr) | Pt (ppm) | DBPMH (g) |
|---|---|---|---|---|
| SR | 137 | 0 | 0 | 2.06 |
| SR/Pt | 137 | 0 | 8 | 2.06 |
| SR/PSiN | 137 | 1.8 | 0 | 2.06 |
| SR/Pt/PSiN | 137 | 0.6–3.6 | 8 | 2.06 |
| SR/Pt/PSiN2 | 137 | 1.8 | 8 | 2.06 |
| SR/Pt/PSiN3 | 137 | 3.0 | 8 | 2.06 |

[a] PSiN = polysilazane, DBPMH = 2,5-bis(*tert*-butylperoxy)-2,5-dimethylhexane.

The tracking and erosion resistance of the silicone rubber was evaluated using an IPT tracking and erosion test apparatus (DX-8427; Dongguan Daxian Instrument Co. Ltd, China), according to IEC 60587. As shown in the schematic of the apparatus (Fig. 2), the specimen was fixed at an angle of 45° by a high-voltage electrode and a ground electrode, spaced 50 mm apart. During the testing, the voltage applied through the electrodes was 4.5 kV. Meanwhile, a standardised 0.1 wt% ammonium chloride and 0.04 wt% iso-octylphenoxypolyethoxyethanol solution dropped into high-voltage electrode at 0.6 mL min$^{-1}$ and flowed across the surface of each specimen into ground electrode by gravity. Five specimens were used for each test. And each test lasted for a maximum time of 6 hours. During the 6 hours, the current on the surface of the specimen was monitored. Once the current exceeded 60 mA for 2 s, the specimen was marked with failure time. The decreased mass of the specimen after IPT was calculated as eroded mass.

Thermogravimetric analysis (TG209F3; Netzsch Instruments Co., Germany) was carried out from 35 °C to 700 °C at a heating rate of 20 °C min$^{-1}$ on 5–10 mg of samples in an $Al_2O_3$ crucible under a 50 mL min$^{-1}$ synthetic air flow comprising 79% nitrogen gas and 21% oxygen gas.

TG-FTIR was adopted to test the pyrolysis gases of the silicone rubber specimens. About 15 mg of silicone rubber sample was placed in an analyser (TG209; Netzsch Instruments Co., Germany). The sample was then heated from 35 °C to 700 °C at a linear rate of 20 °C min$^{-1}$ under a synthetic air flow. During heating, the pyrolysis gases were continuously transferred through a 1 mm inner-diameter tube with a temperature of 230 °C to an FTIR spectrometer (Tensor 27; Bruker Optics, Germany).

SEM (EVO18, Zeiss, Germany) was used to observe the morphology of the silicone rubber samples after IPT. A thin layer of gold was sprayed on the surface of the samples before observation. The acceleration voltage was 10.0 kV.

LRS, using a Raman microspectrometer (Horiba LabRAM; HR Evolution, France) with a 532 nm helium–neon laser source and a range of 50 to 2000 cm$^{-1}$, was conducted on the silicone rubber samples after the IPT.

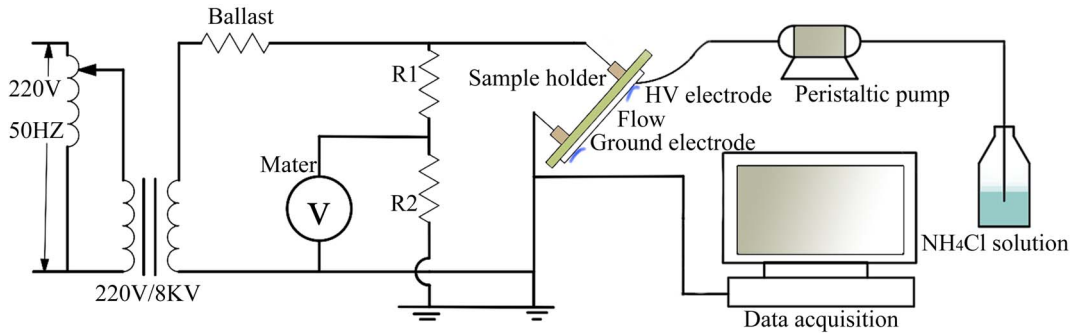


Fig. 2 Schematic of the inclined plane test.

## Results and discussion

### Tracking and erosion resistance

The results of IPTs are shown in Fig. 3, and photographs of the specimens after testing are presented in Fig. 4. The results indicated that when the PSiN content was ≤1.2 phr, all the specimens failed within 360 min due to excess leakage current. In addition, these specimens formed carbonaceous tracking roads that linked the high-voltage and ground electrodes, which acted as leakage-current carriers (Fig. 4). However, when the PSiN content was between 1.8 and 2.4 phr, the specimens passed the IPT and exhibited low eroded masses. Furthermore, the surfaces of these specimens were almost undamaged after the 4.5 kV IPT (Fig. 4). This indicated excellent tracking and erosion resistance, attributed to the cooperation and synergistic effect of adequate PSiN and Pt contents. It is assumed that a densely crosslinked network catalysed by PSiN/Pt was developed, which protected the inner materials from arc damage.[22,25] With PSiN contents of ≥3.0 phr, the specimens did not exhibit excess leakage current, but they tended to exhibit high eroded masses that corresponded to a high depth of damage (Fig. 3 and 4). It might be that PSiN could transfer into inorganic structure at high temperature.[26] Therefore, excess PSiN content resulted in production of erosion compound at hot spot, under arc discharging.

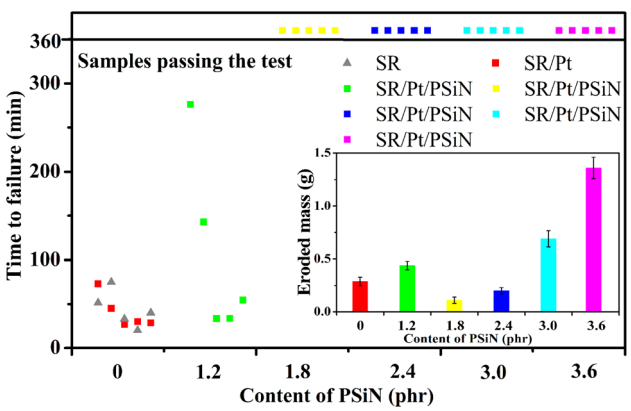


Fig. 3 Effect of polysilazane (PSiN) content on the result of the inclined plane test at 4.5 kV for silicone rubber specimens.

### Thermogravimetric analysis

The tracking and erosion of silicone rubber are mainly attributed to thermal degradation induced by arcing.[27] Thus, high thermal stability is key for developing silicone rubber with excellent tracking and erosion resistance. The TG and derivative

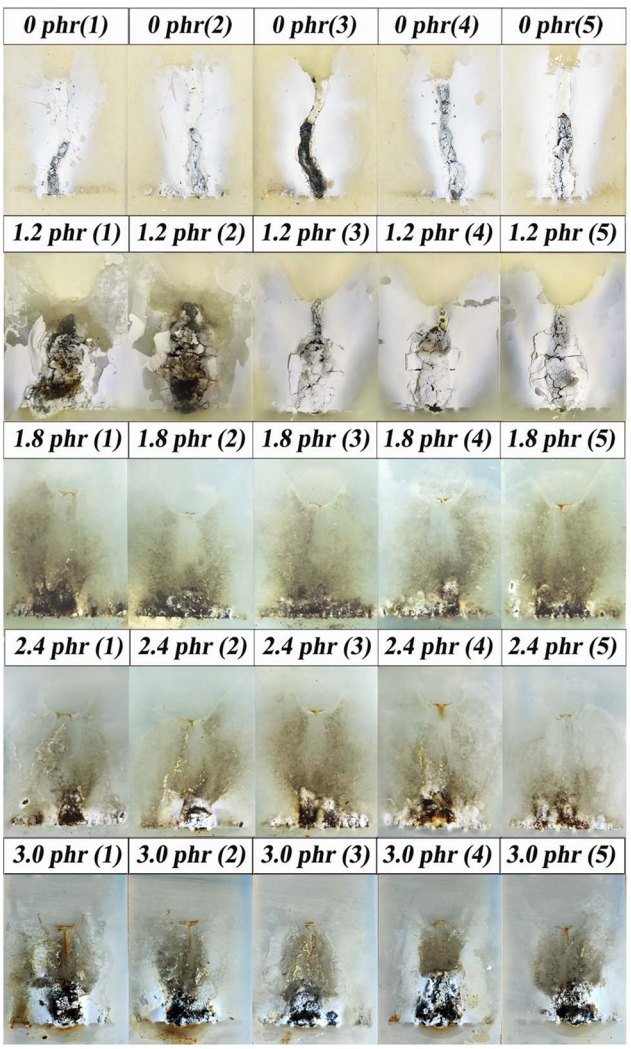


Fig. 4 Photographs of the silicone rubber specimens after the inclined plane test at 4.5 kV.

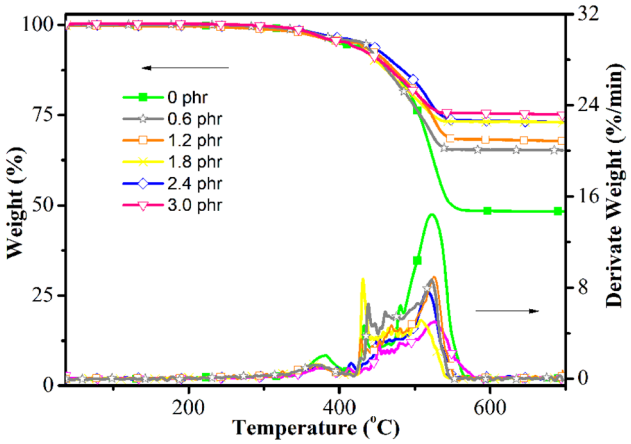


Fig. 5 Thermogravimetric curves of silicone rubbers.

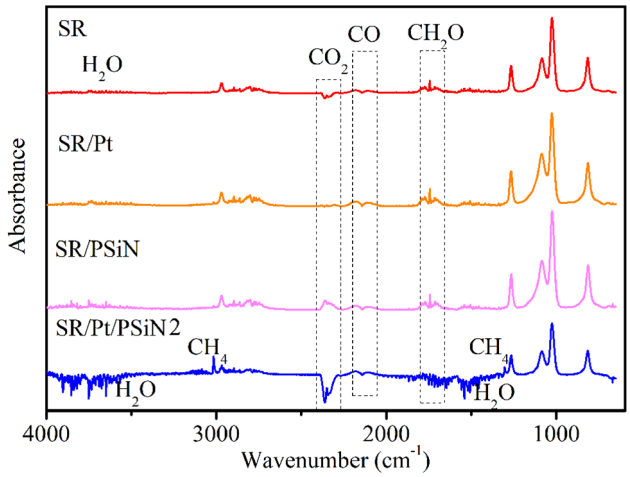


Fig. 6 Fourier transform infrared spectrometry spectra of pyrolysis gases at maximum release during thermal degradation of silicone rubbers.

Table 2 Effect of PSiN content on the thermal degradation characteristics of silicone rubbers

| PSiN content (phr) | $T_{10}$ (°C) | $T_{20}$ (°C) | $R_{max}$ (wt%/min) | Residue weight at 700 °C (wt%) |
|---|---|---|---|---|
| 0.0 | 453 | 495 | 14.4 | 48.0 |
| 0.6 | 454 | 491 | 8.67 | 65.2 |
| 1.2 | 461 | 506 | 8.95 | 67.7 |
| 1.8 | 449 | 499 | 8.76 | 73.0 |
| 2.4 | 469 | 516 | 7.74 | 73.0 |
| 3.0 | 413 | 455 | 5.14 | 75.1 |

TG curves of silicone rubbers with different PSiN contents are shown in Fig. 5, and their characteristic data are shown in Table 2. This shows that the temperature at 10 wt% loss ($T_{10}$) and the temperature at 20 wt% loss ($T_{20}$) of the silicone rubber showed small changes after adding 0–2.4 phr of PSiN. Silicone rubber with 3 phr of PSiN showed decreased $T_{10}$ and $T_{20}$, which could lead to reduced erosion resistance. However, the maximum degradation rate ($R_{max}$) decreased with increasing PSiN. Therefore, the residue at 700 °C was significantly increased for silicone rubber containing PSiN. This high thermal residue might have contributed to the improved tracking resistance.

### TG-FTIR analysis

To determine the effects of PSiN and Pt on the thermal degradation of silicone rubber, TG-FTIR was used to test the pyrolysis gases of the silicone rubber specimens. The FTIR spectra of the pyrolysis gases at maximum release during the thermal degradation of the specimens are shown in Fig. 6. These indicated that the main pyrolysis products of the silicone rubber specimens were cyclic oligomers (816, 1026, 1086, 1265 and 2970 $cm^{-1}$), which originated from the degradation of the silicone chains.[28] Additionally, oxidation products, including $CH_2O$ (carbonyl compounds, 1745 $cm^{-1}$), CO (2181 and 2114 $cm^{-1}$), $CO_2$ (2360 and 2341 $cm^{-1}$) and $H_2O$ (3500–3700 and 1541 $cm^{-1}$), were also detected during the thermal degradation.[28] Besides, $CH_4$ (methane; 3016 and 1306 $cm^{-1}$) was detected for SR/Pt/PSiN during thermal degradation.

The thermal degradation of the silicone rubber mainly followed three mechanisms: molecular mechanism, radical mechanism and unzipping depolymerisation.[28] As demonstrated in Fig. 7a and b, the molecular mechanism and unzipping depolymerisation resulted in the degradation of the silicone chains by the constant removal of cyclic oligomers. The action of oxygen transformed Si–$CH_3$ into Si–OH and released $CH_2O$, as shown in Fig. 7b. Si–OH easily induced unzipping depolymerisation and meantime the oxidative crosslinking of silicone chains occurs *via* the dehydration condensation of Si–OH. In addition, the high temperature induced the radical mechanism (Fig. 7c) in the silicone chains, which caused radical crosslinking and generated $CH_4$. Furthermore, the oxidation of the cyclic oligomers, $CH_2O$ and $CH_4$ generated CO, $CO_2$ and $H_2O$. Fig. 6 shows that SR/Pt/PSiN contained lower amounts of cyclic oligomers and $CH_2O$ but higher amounts of $CO_2$ and $CH_4$ than SR, SR/Pt and SR/PSiN. This meant that the combined addition of PSiN and Pt facilitated the radical mechanism and suppressed the unzipping depolymerisation and molecular mechanism in the silicone chains. Thus, the degradation of silicone chains was retarded by the presence of PSiN and Pt.

Fig. 8 shows the evolution of the main absorbance peaks of the pyrolysis gases as a function of temperature, that is, the absorbance of $CH_2O$ (1745 $cm^{-1}$), cyclic oligomers (1026 $cm^{-1}$) and $CH_4$ (3016 $cm^{-1}$). $CH_2O$ emerged first, which suggested the oxidation of silicone chains (Fig. 7b). Then, cyclic oligomers started evolving at 350 °C, which suggested the degradation of silicone chains. $CH_4$ was detected above 440 °C. It was indicated that adding PSiN or Pt alone increased the release of $CH_2O$ and cyclic oligomers. This also suggested that the addition of PSiN or Pt alone accelerated the oxidation and degradation of the silicone chains. However, the combined addition of PSiN and Pt decreased the release of $CH_2O$ and cyclic oligomers. This

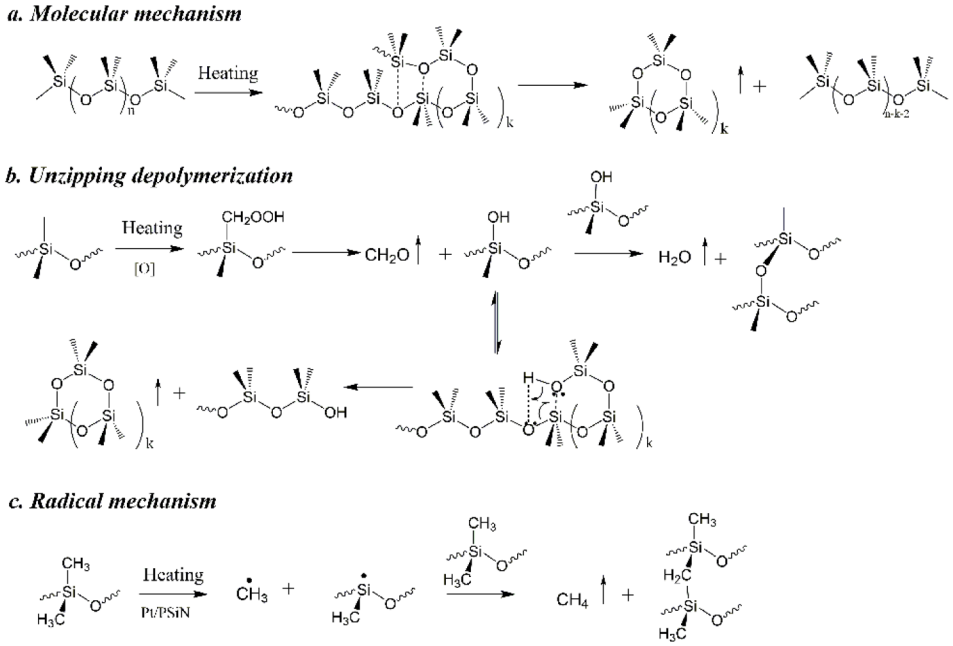


Fig. 7 Thermal degradation mechanisms of silicone rubber: (a) molecular mechanism; (b) unzipping depolymerization; (c) radical mechanism.

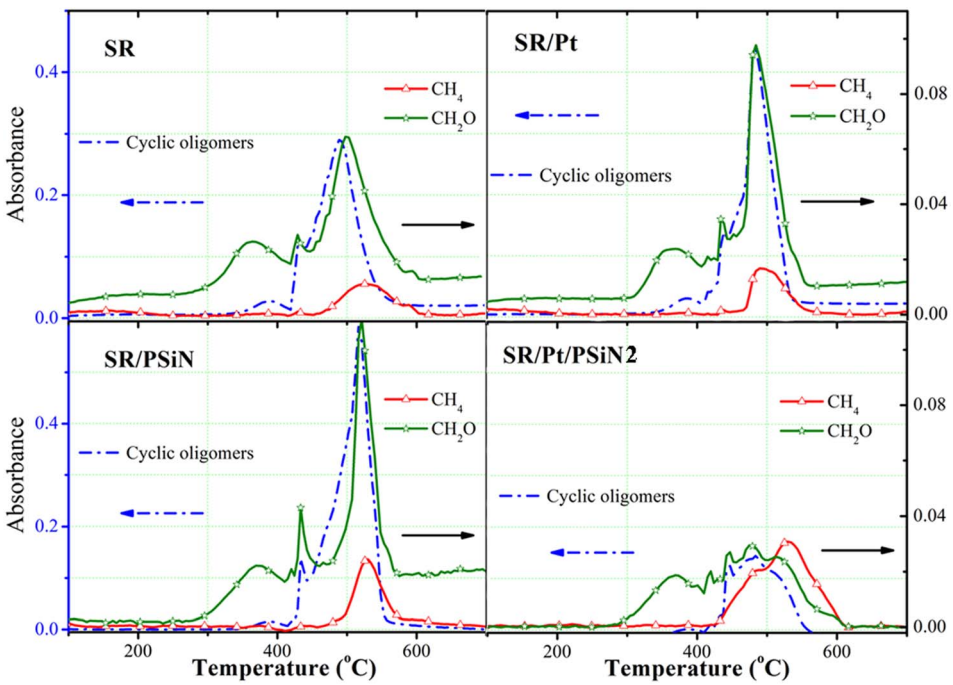


Fig. 8 Fourier transform infrared spectrometry absorbance of characteristic peaks of pyrolysis gases *versus* temperature during thermal degradation of silicone rubbers.

suggested that the oxidation and degradation of the silicone chains were significantly suppressed due to the synergistic action of PSiN and Pt. The release of $CH_4$ increased slightly after adding PSiN or Pt alone. Nevertheless, the combined addition of PSiN and Pt led to a significant increase in the release of $CH_4$. This indicated that the synergistic action of PSiN and Pt significantly enhanced the radical mechanism. The nitrogen atom in PSiN could coordinate with Pt atom through lone pair electrons, which inhibited Pt aggregation and retained the catalytic activity of Pt at high temperature.[29] Thus, a tight crosslinked network was catalysed and formed due to the action of Pt/PSiN, which effectively resisted the degradation of the

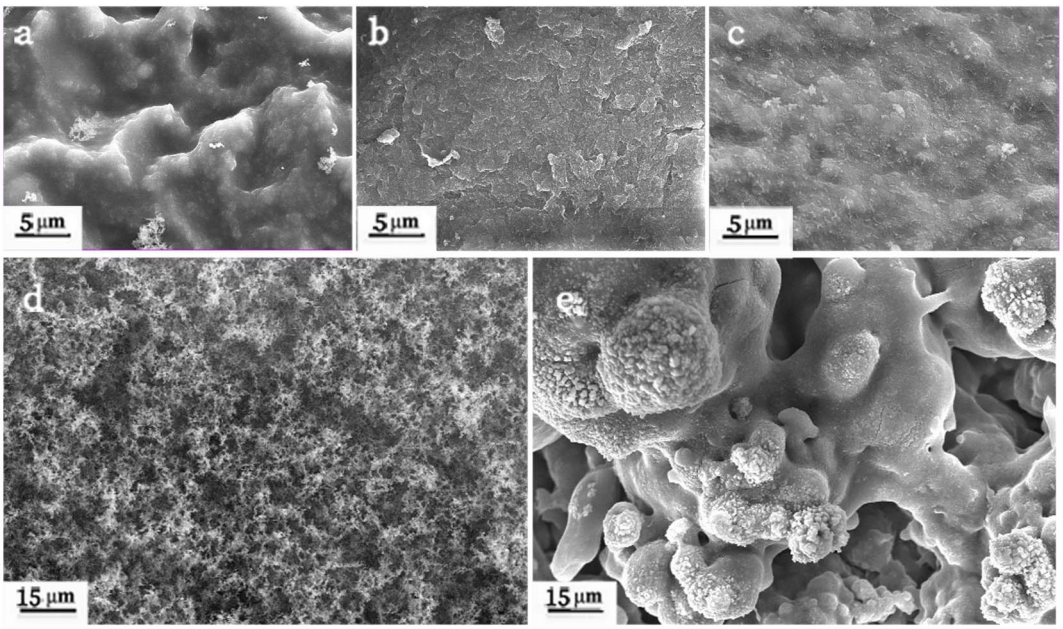


Fig. 9 Scanning electron microscopy images of silicone rubber specimens after inclined plane test: (a) the surface under tracking compound for SR; (b) the most damaged area for SR/Pt/PSiN2; (c) the surface under erosion compound for SR/Pt/PSiN3; (d) tracking compound for SR; (e) erosion compound for SR/Pt/PSiN3.

silicone chains and contributed to excellent tracking and erosion resistance.

### Morphological analysis of the residues

SEM images of the silicone rubber specimens after IPT are shown in Fig. 9. The silicone rubber without PSiN (Fig. 9a) had a rough and uneven surface due to arcing damage. In the presence of 1.8 phr PSiN and Pt, the silicone rubber had a flat and undamaged surface, which suggested excellent tracking and erosion resistance (Fig. 9b). Nevertheless, when the PSiN content reached 3 phr, the silicone rubber exhibited an undulating surface (Fig. 9c) due to arc erosion. Fig. 9d and e show the morphologies of a black tracking compound and an erosion compound that originated from silicone rubber contained 0 phr and 3 phr PSiN, respectively. The tracking compound was loose and porous; however, the erosion compound was dense and tough. It might be that the synergistic action of PSiN and Pt catalysed crosslinking of silicone chains. A highly crosslinked network further facilitated the transition of PSiN into tough inorganic substances.[24]

### LRS analysis

To investigate the components of the silicone rubber specimens after the IPT, LRS was applied to characterise the residues. Fig. 10 shows the LRS spectra of the tracking compound for SR, the SR/Pt/PSiN3 erosion compound and the passed SR/Pt/PSiN2 specimens. The tracking compound exhibited the obvious carbon characteristic peaks of G (1596 $cm^{-1}$) and D bands (1297 $cm^{-1}$), which implied the production of conductive carbon and accounted for the tracking roads.[30] The erosion compound showed Si–O stretching peaks (481 $cm^{-1}$), $SiC_2$ symmetric stretch (691 $cm^{-1}$) and a weak D band peak.[31] This suggested that the addition of PSiN and Pt suppressed the pyrolysis of silicone chains into carbon. Furthermore, SR/Pt/PSiN2 only showed Si–O stretching and $SiC_2$ symmetric stretching peaks. This indicated that the structures of the silicone chains were not destroyed for SR/Pt/PSiN2 after IPT. Thus, an appropriate PSiN content contributed to the excellent tracking and erosion resistance of the silicone rubber.

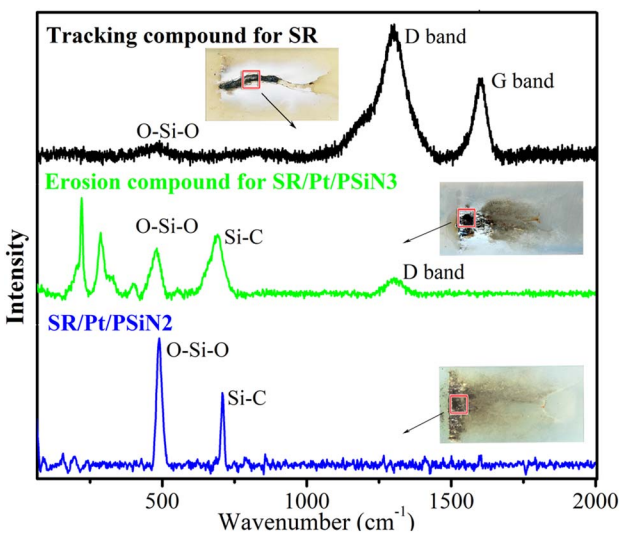


Fig. 10 Laser Raman spectroscopy spectra of silicone rubbers after inclined plane test.

**Suppression mechanism**

A suppression mechanism for PSiN/Pt on tracking and erosion of silicone rubber was proposed. Due to the high temperature produced by arc discharge, silicone chains suffer from thermal oxidation and degradation. They are also pyrolysed to produce conductive carbon, which constitutes the tracking road. However, the presence of PSiN/Pt suppresses the thermal oxidation and degradation of silicone chains. In addition, the radical crosslinking of silicone chains is catalysed by PSiN/Pt. Thus, a tightly crosslinked network is formed to resist arc ablation. Furthermore, PSiN/Pt suppresses the generation of carbon deposits. Thus, tracking and erosion resistance are improved for SR/Pt/PSiN.

## Conclusions

PSiN and Pt effectively improved the tracking and erosion resistance of silicone rubber. After adding 1.8–2.4 phr of PSiN and 8 ppm of Pt, the silicone rubber passed the 4.5 kV IPT. The eroded mass also largely decreased, and the surface was undamaged after IPT. The TG test showed that PSiN and Pt significantly improved the thermal stability of the silicone rubber, which led to a significantly decreased maximum degradation rate and a high residue (73 wt%) at 700 °C. TG-FTIR and SEM indicated that PSiN/Pt effectively catalysed the radical crosslinking of silicone chains induced by high temperatures. As a result, a protective barrier was developed to resist arc ablation and thermal degradation. Furthermore, LRS suggested that appropriate amounts of added PSiN and Pt suppressed the production of conductive carbon and thus prevented tracking.

## Author contributions

W. Chen and M. Zhang supervised the work. Z. S. Li and S. Y. Mai prepared silicone rubber specimens. J. W. Zheng and Y. Cai performed the IPT, TG test, TG-FTIR measurements, SEM observation and LRS measurements. All authors contributed to the scientific discussion and manuscript preparation. W. Chen wrote the manuscript. All authors have read and agreed to the published version of the manuscript.

## Conflicts of interest

There are no conflicts to declare.

## Acknowledgements

The authors kindly acknowledge the financial support of the National Natural Science Foundation of China (No. 52103107), the Guangdong Basic and Applied Basic Research Foundation (2019A1515111049), the High-Level Talent Start-Up Research Project of Foshan University (gg07093) and Foshan Functional Polymer Engineering Center (No. 2016GA10162).

## Notes and references

1 M. Z. Saleem and M. Akbar, *Polymers*, 2022, **14**, 431.
2 D. Ghosh, S. Bhandari, T. K. Chaki and D. Khastgir, *RSC Adv.*, 2015, **5**, 57608–57618.
3 D. A. Bolliger and S. A. Boggs, *IEEE Trans. Dielectr. Electr. Insul.*, 2012, **19**, 996–1006.
4 C. Chen, Z. Jia, X. Wang, H. Lu, Z. Guan and C. Yang, *IEEE Trans. Dielectr. Electr. Insul.*, 2015, **22**, 313–321.
5 C. Xu, R. Guan, Z. Jia, X. Wang and Y. Deng, *IEEE Trans. Dielectr. Electr. Insul.*, 2022, **29**, 1974–1982.
6 S. M. Rowland, G. P. Bruce, L. Yuting, A. Krivda and L. E. Schmidt, *IEEE Trans. Dielectr. Electr. Insul.*, 2011, **18**, 365–374.
7 S. Sun, M. Zhao, F. Chen, Z. Wu and J. Wang, *IEEE Trans. Dielectr. Electr. Insul.*, 2022, **29**, 933–938.
8 R. A. Ghunem, E. A. Cherney and S. H. Jayram, *IEEE Trans. Dielectr. Electr. Insul.*, 2021, **28**, 1636–1642.
9 S. Ilhan, D. Tuzun and A. Ozdemir, *IEEE Trans. Dielectr. Electr. Insul.*, 2021, **28**, 414–422.
10 R. A. Ghunem, S. Ilhan, H. I. Uckol, D. Tuzun and Y. Hadjadj, *IEEE Trans. Dielectr. Electr. Insul.*, 2021, **28**, 2144–2151.
11 A. Y. Alqudsi, R. A. Ghunem and E. David, *IEEE Trans. Dielectr. Electr. Insul.*, 2022, **29**, 1873–1881.
12 B. Venkatesulu and M. J. Thomas, *IEEE Trans. Dielectr. Electr. Insul.*, 2010, **17**, 615–624.
13 B. X. Du and X. Hang, *IEEE Trans. Dielectr. Electr. Insul.*, 2014, **21**, 511–518.
14 A. Y. Alqudsi, R. A. Ghunem and E. David, *IEEE Trans. Dielectr. Electr. Insul.*, 2021, **28**, 788–796.
15 M. T. Nazir, B. T. Phung, S. Yu and S. Li, *IEEE Trans. Dielectr. Electr. Insul.*, 2018, **25**, 2076–2085.
16 R. A. Ghunem, D. Kone, L. Cisse, Y. Hadjadj, H. Parks and D. Ambroise, *IEEE Trans. Dielectr. Electr. Insul.*, 2020, **27**, 249–256.
17 S. Ansorge, F. Schmuck and K. Papailiou, *IEEE Trans. Dielectr. Electr. Insul.*, 2015, **22**, 979–988.
18 Z. An, Y. Qin, T. Chen and J. Xu, *IEEE Trans. Dielectr. Electr. Insul.*, 2022, **29**, 1685–1692.
19 L. Schmidt, X. Kornmann, A. Krivda and H. Hillborg, *IEEE Trans. Dielectr. Electr. Insul.*, 2010, **17**, 533–540.
20 W. Fang, X. Lai, H. Li, W. Chen, X. Zeng, L. Zhang and S. Yang, *Polym. Test.*, 2014, **37**, 19–27.
21 C. Xie, X. Lai, H. Li and X. Zeng, *Polym. Degrad. Stab.*, 2021, **188**, 109565.
22 W. J. Chen, X. Zeng, X. Lai, H. Li, W. Z. Fang and F. Hou, *ACS Appl. Mater. Interfaces*, 2016, **8**, 21039–21045.
23 Y. L. Wang, F. Qian, X. J. Lai, H. Q. Li, X. R. Zeng, Z. Y. Liu and J. F. Gao, *Composites, Part B*, 2022, **245**, 110200.
24 W. Chen, X. Zhang, C. Liang, D. Chen, M. Zhang and L. Miao, *J. Elastomers Plast.*, 2021, **54**, 359–373.
25 E. Delebecq, S. Hamdani-Devarennes, J. Raeke, J. M. Lopez Cuesta and F. Ganachaud, *ACS Appl. Mater. Interfaces*, 2011, **3**, 869–880.
26 L. Ribeiro, O. Flores, P. Furtat, C. Gervais, R. Kempe, R. Machado and G. Motz, *J. Mater. Chem. A*, 2017, **5**, 720–729.
27 Y. Liu, D. Zhang, H. Xu, S. M. Ale-Emran and B. X. Du, *IEEE Trans. Dielectr. Electr. Insul.*, 2016, **23**, 2102–2109.
28 W. Chen, X. Zeng, X. Lai, H. Li, W. Fang and T. Liu, *Thermochim. Acta*, 2016, **632**, 1–9.

29 T. Liu, X. Zeng, X. Lai, H. Li and Y. Wang, *Polym. Degrad. Stab.*, 2020, **171**, 109026.
30 J. Han, G. Liang, A. Gu, J. Ye, Z. Zhang and L. Yuan, *J. Mater. Chem. A*, 2013, **1**, 2169–2182.
31 A. Labouriau, C. Cady, J. Gill, J. Stull, D. Ortiz-Acosta, K. Henderson, V. Hartung, A. Quintana and M. Celina, *Polym. Degrad. Stab.*, 2015, **116**, 62–74.